Hindawi Publishing Corporation
Journal of Nanomaterials
Volume 2015, Article ID 921394, 14 pages
http://dx.doi.org/10.1155/2015/921394

Research Article

Comparative Studies on Thermal Performance of Conic Cut Twist Tape Inserts with SiO_2 and TiO_2 Nanofluids

Sami D. Salman,[1,2] Abdul Amir H. Kadhum,[1] Mohd S. Takriff,[1] and Abu Bakar Mohamad[1]

[1]*Department of Chemical and Process Engineering, Faculty of Engineering and Built Environment, Universiti Kebangsaan Malaysia, 43600 Bangi, Selangor, Malaysia*
[2]*Biochemical Engineering Department, Al-khwarizmi College of Engineering, University of Baghdad, Baghdad 47024, Iraq*

Correspondence should be addressed to Sami D. Salman; sami.albayati@gmail.com

Received 20 August 2014; Revised 21 October 2014; Accepted 28 October 2014

Academic Editor: Rupesh S. Devan

This paper presents a comparison study on thermal performance conic cut twist tape inserts in laminar flow of nanofluids through a constant heat fluxed tube. Three tape configurations, namely, quadrant cut twisted tape (QCT), parabolic half cut twisted tape (PCT), and triangular cut twisted (VCT) of twist ratio $y = 2.93$ and cut depth $d_e = 0.5$ cm were used with 1% and 2% volume concentration of SiO_2/water and TiO_2/water nanofluids. Typical twist tape with twist ratio of $y = 2.93$ was used for comparison. The results show that the heat transfer was enhanced by increasing of Reynolds number and nanoparticles concentration of nanofluid. The results have also revealed that the use of twist tape enhanced the heat transfer coefficient significantly and maximum heat transfer enhancement was achieved by the presence of triangular cut twist tape insert with 2% volume concentration of SiO_2 nanofluid. Over the range investigated, the maximum thermal performance factor of 5.13 is found with the simultaneous use of the SiO_2 nanofluid at 2% volume concentration VCT at Reynolds number of 220. Furthermore, new empirical correlations for Nusselt number, friction factor, and thermal performance factor are developed and reported.

1. Introduction

Heat transfer enhancement technique plays substantial role for laminar flow regime, due to the deficiency of heat transfer coefficient in plain tubes. Heat transfer augmentation techniques can be classified as active and passive techniques [1, 2]. Active techniques require external power source, such as electric field, surface vibration, or Jet impingement. Whereas, passive techniques require fluid additives, surface modifications, or swirl/vortex flow devices to enhance heat transfer. The swirl flow devices include coil wire, helical wire coil, and twist tape inserts. So, many published articles related to experimental and numerical investigation on convective heat transfer using twisted tape inserts and water as test fluid have been reported in the literature [3–13]. The limitation of thermophysical properties and low thermal conductivity of water led to innovative new fluid which can enhance the heat transfer. Small amount of nanoparticles was dispersed into base fluid to improve its thermal conductivity. The resultant fluid of suspended nanoparticles into base fluid was called nanofluid. Nanofluids were first used by Choi and Eastman [14] in 1995 at Argonne National Laboratory, USA. Subsequently, several types of nanoparticles have been employed for nanofluid preparation, including metals such as gold (Au), copper (Cu), and silver (Ag) and also metal oxides such as TiO_2, Fe_3O_4, Al_2O_3, and CuO [15–21]. Due to their significantly lower cost, metal oxides are preferred for heat transfer enhancement application compared to metals. The combination between twisted tape inserts with nanofluids was simultaneously utilized to produce heat transfer enhancement greater than either techniques operating individually. Pathipakka and Sivashanmugam [22] proposed CFD simulation for laminar heat transfer characteristics using Al_2O_3/water nanofluids in a uniform heat fluxed tube equipped with helical twist tape inserts. Twist tape of twist ratios 2.93, 3.91, and 4.89 with three different volume concentrations of 0.5%, 1%, and 1.5% Al_2O_3/water was simultaneously used for simulation. The maximum heat

transfer enhancement of 31.29% was obtained with the use of helical insert of twist ratio 2.93 together with nanofluid with volume concentration of 1.5% at Reynolds number of 2039. Wongcharee and Eiamsa-ard [23] have investigated heat transfer, friction, and thermal performance characteristics of CuO/water nanofluids in a circular tube fitted with alternate axis and the typical twisted tapes experimentally. Three different volume concentrations of 0.3%, 0.5%, and 0.7% CuO/water with twisted tapes at constant twist ratio y/w = 3 were used for investigation. Their results revealed that maximum thermal performance factor of 5.53 was obtained at Reynolds number of 1990 with the simultaneous use of 0.7% CuO/water nanofluid with alternate axis twisted tape. Suresh et al. [24] have performed a comparative study on the thermal performance of helical screw tape inserts with 0.1% volume concentration Al_2O_3/water and CuO/water nanofluids in laminar flow through a straight circular duct under constant heat flux boundary condition. The helical screw tape inserts with twist ratios y = 1.78, 2.44, and 3 were used for investigation. The experimental results show that the helical screw tape inserts offered better thermal performance factor when used with CuO/water nanofluid than with Al_2O_3/water nanofluid. Salman et al. [25] reported numerical study on heat transfer enhancement of CuO/water nanofluid in a constant heat fluxed tube fitted with classical and one side parabolic-cut twist tape inserts using FLUENT version 6.3.26. Twisted tapes of different twist ratios (y = 2.93, 3.91, and 4.89) and different cut depths (w = 0.5, 1, and 1.5 cm) were simultaneously used with 2% and 4% volume concentration CuO nanofluid for simulation. Their results elaborated that the parabolic cut twist tape of twist ratio y = 2.93 and cut depth w = 0.5 with 4% CuO nanofluid offers about 10% enhancement for the Nusselt number than that of classical twisted tape at the same conditions. Salman et al. [26] reported an application of a mathematical model of the heat transfer enhancement and friction factor characteristics of water in constant heat-fluxed tube fitted with one side elliptical cut twisted tape inserts with twist ratios (y = 2.93, 3.91, and 4.89) and different cut depths (w = 0.4, 0.8, and 1.4 cm) under laminar flow using FLUENT version 6.3.26. The results elaborated that the enhancement of heat transfer rate and the friction factor induced by elliptical cut twisted tape inserts increases with the Reynolds number and decreases with twist ratio. In addition, the results show that the elliptical cut twisted tape with twist ratio y = 2.93 and cut depth w = 0.5 cm offered higher heat transfer rate with significant increases in friction factor. Salman et al. [27] also studied heat transfer of water in a uniformly heated circular tube fitted with one side quadrant cut twisted tape inserts in laminar flow using FLUENT version 6.3.26. Classical and quadrant cut twisted tape with twist ratio (y = 2.93, 3.91, and 4.89) and different cut depths (w = 0.5, 1, and 1.5 cm) were employed for the simulation. The results show that the quadrant cut twisted tape with twist ratio (y = 2.93) and cut depth (w = 0.5 cm) presents a maximum heat transfer rate with significant increases in friction factor. The attractive characteristics of triangular, elliptic, and quadrant cut twist tape with twist ratio y = 2.93, mentioned above, have motivated the present research to combine the effects of a novel tube insert with the laminar flow of nanofluids. For the present study, an experimental comparison study on the thermal performance of alternative conic cut twist tape inserts with SiO_2/water and TiO_2/water nanofluids in uniform heat fluxed tube was implemented. The tests using nanofluid with and without typical twisted tape were also conducted, for comparison.

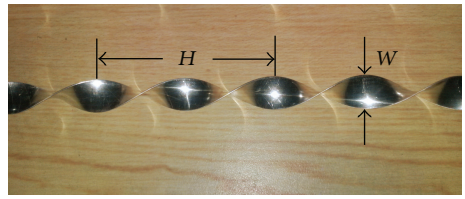

Figure 1: Typical twisted tape (TT).

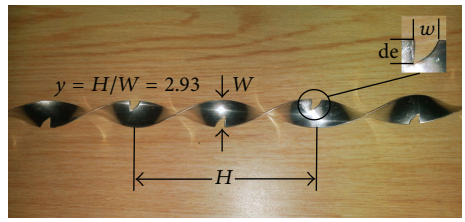

Figure 2: Quadrant cut twisted tape (QCT).

2. Technical Details of Twisted Tape Inserts

The geometrical configuration of typical and conic-cut twist tape inserts is shown in Figures 1, 2, 3, and 4. Aluminium strips of 0.8 mm thickness, 24.5 mm width, and 1800 mm length are uniformly winding over a specified distance of 75 mm to produce the desired twist ratio (y = 2.93). The twist ratio "y" was defined as the ratio of the length of one full twist (360°) to the tape width. The conic cut shapes are drawn for the specified distance on the strips before twisting. Thereafter, cuts are made on twisted tape based on these cut shapes to obtain the desired configurations.

3. Nanofluid Properties

The silica and titanium oxide nanoparticles delivered from US Research Nanomaterials Inc. with properties illustrated in Table 1 were used for nanofluids preparation of the nanofluid. The particle size and chemical composition of nanoparticles were checked before nanofluid samples preparation. Field Emission Scanning Electron Microscopy (FESEM) was used for particle size, shape, and agglomeration visualization. The FESEM results show that the nanoparticles are in approximately spherical shape with diameter around 20 nm. Energy-dispersive X-ray spectroscopy (EDX) was used for elemental analysis or chemical characterization. The EDX spectrum of nanoparticles is shown in Figures 5 and 6. Nanofluids with desired volume concentrations of 1% and 2% were prepared by dispersing specified amounts of SiO_2 and TiO_2 nanoparticles in deionised water. The samples were agitated

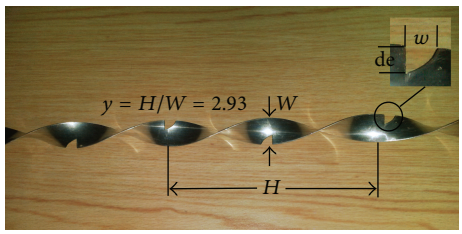

Figure 3: Parabolic half cut twisted tape (PCT).

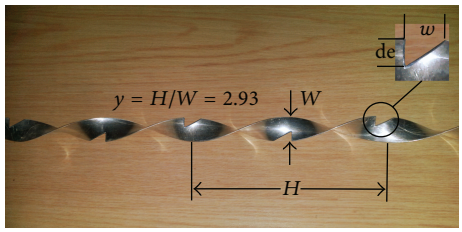

Figure 4: Triangular cut twist tape (VCT).

Table 1: Properties of nanoparticles at 20°C.

Material	Density (gm/cm^3)	Specific heat (MJ/m^3 K)	Thermal conductivity (W/m K)	Particle size (nm)
SiO_2	2.2	745	1.4	15–20
TiO_2	3.9	650	11.2	15–20

Table 2: Thermophysical properties of water and nanofluids at 25°C.

Fluid	Density ρ (gm/cm^3)	Viscosity μ (Ns/m^2)	Specific heat (MJ/m^3·K)	Thermal conductivity (W/m·K)
Water	0.9969	0.000963	4.1672	0.6096
Water + 1% SiO_2	1. 0090	0.001068	4.1412	0.6275
Water + 2% SiO_2	1.0211	0.001197	4.1141	0.6288
Water + 1% TiO_2	1.0260	0.001073	4.1483	0.6455
Water + 2% TiO_2	1.0550	0.001188	4.1415	0.6672

for 1 hr and finally transferred to Ultrasonic bath (NEY-280H) for 1 hour in order to break up any potential clusters of nanoparticles and to achieve the required homogeneous suspensions. The thermophysical properties of nanofluids for desired volume concentration ϕ were measured 25°C using portable density meter (Type DA-130N), POLYVISC rotational viscometer, and Hot Disk Transient Plane Source TPS 2500S. Properties of the water and nanofluids are shown in Table 2.

4. Experimental Setup

The experimental set-up as shown in Figure 7 consists of a test section, calming section, chilled water tank with cooling unit, circulation pump, and pipe line system. Both the calming section and test sections are made of straight stainless steel tube

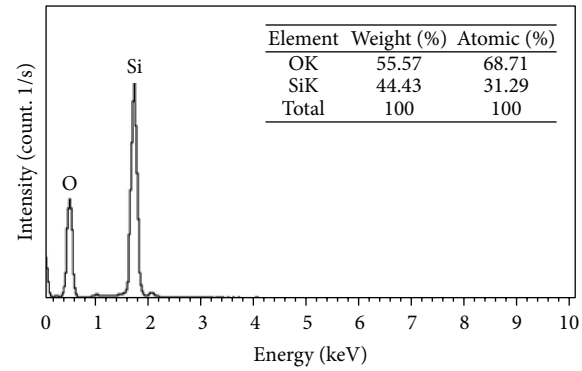

Figure 5: EDX spectrum of SiO_2 nanoparticles.

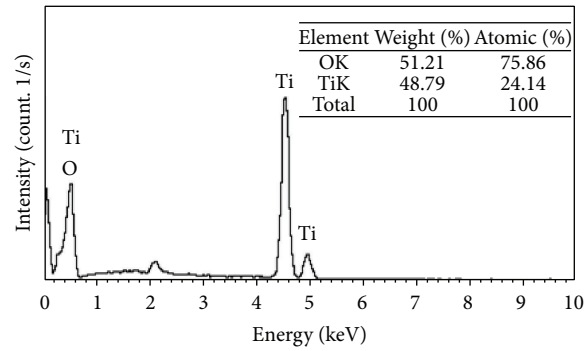

Figure 6: EDX spectrum of TiO_2 nanoparticles.

with the dimensions 2000 and 1800 mm long, respectively, with 25.4 mm ID and 33.33 mm OD. The calming section is used to eliminate the entrance effect. The outside surface of the test section is brazed with fifteen thermowells made of stainless steel with dimensions of 6.36 mm ID, 1 mm thick, and 120 mm length which are mounted on the test section at axial positions as shown in Figure 8. The test section tube is wound with ceramic beads coated electrical SWG Nichrome heating wire of resistance 18 Ω. Over the electrical winding, two layers of asbestos rope and glass wool insulations are used to minimize heat loss. The terminals of the Nichrome wire are attached to the Volteq 3 KVA variac variable transformer with input single phase 220 V AC, 50 Hz and output voltage can be adjusted from 0 to 150 V AC. The amount of heat required in test section can be achieved by varying the output voltage. Fifteen calibrated RTD PT 100 type temperature sensors with 0.75% accuracy are placed in the thermowells to measure the outside wall temperatures. Two RTD PT 100 type temperature sensors are inserted near the centre of pipe to measure the bulk temperature of fluid at inlet and outlet of test section. The pressure drop across the test section is measured using DMP3051 digital on-line differential pressure transmitter and the velocity of water and nanofluids is measured by portable TDS-100H ultrasonic flowmeter. The hot fluid after passing through the heated test section flows through chilled water for cooling and the desired temperature is controlled by temperature controller. 30 m head centrifugal pump with by-pass valves is used to regulate the flow rate through the

Table 3: Technical details of experimental setup and test conditions.

Setup and conditions	Description
(A) Experimental setup	
(a) Inner tube inner diameter (di)	25.40 mm
(b) Outer tube inner diameter (do)	33.35 mm
(c) Test tube length	1800 mm
(d) Material of inner tube	Stainless steel 304L
(f) Insulation material	Asbestos rope and glass wool
(g) Temperature measurements	RTD Pt 100 type (±0.75% accuracy)
(h) Flow measurements	TDS-100H ultrasonic flowmeter (±0.1% accuracy)
(i) Pressure measurement	DMP3051 differential pressure transmitter (±0.2% accuracy)
(k) Heater capacity	3 KW
(B) Typical twisted tape (TT)	
(a) Material	Aluminium
(b) Tape width (W)	24.5 mm
(c) Tape thickness	0.8 mm
(d) Tape pitch length (H, 360°)	75 mm
(e) Twist ratio ($y = H$/di)	2.93
(C) Conic cut twisted tape	
(a) Material	Aluminium
(b) Tape width (W)	24.5 mm
(c) Tape thickness	0.8 mm
(d) Tape pitch length (H, 360°)	75 mm
(e) Twist ratio ($y = H$/di)	2.93
(f) Quadrant cut twist tape (QCT)	w = 5 mm, de = 5 mm
(g) Parabolic cut twist tape (PCT)	w = 5.89 mm, de = 5 mm
(h) Triangular cut twist tape (VCT)	w = 7.85 mm, de = 5 mm
(D) Test conditions	
(a) Reynolds number, (Re)	200 to 1500
(b) Type of flow in inner tube	Laminar

test section. The details of experimental setup and operating conditions are summarized in Table 3.

5. Data Reduction

The measured data were used to calculate the Nusselt number, friction factor, and thermal performance factor in the laminar flow regime for Reynolds number ranging from 200 to 1500.

The heat transfer rate obtained from the hot fluid in the test section tubes can be expressed as

$$Q_{\text{conv}} = mc_p \left(T_{\text{out}} - T_{\text{in}}\right). \tag{1}$$

The heat transfer rate in terms of mean convective heat transfer coefficient (h) can be expressed as

$$Q_{\text{conv}} = hA \left(\widetilde{T}_s - T_b\right). \tag{2}$$

The heat flux becomes

$$q_s'' = \frac{Q_{\text{conv}}}{A} = h\left(\widetilde{T}_s - T_b\right), \tag{3}$$

where T_b is a mean bulk flow temperature $T_b = (T_{\text{out}} + T_{\text{in}})/2$.

Then, mean inner wall surface temperature ($\widetilde{T}_s$) of the test section is calculated from 15 stations of surface temperatures located between the inlet and the outlet of the test section, using the following equation:

$$\widetilde{T}_s = \sum \frac{T_{si}(x)}{15}, \tag{4}$$

where $T_{si}(x)$ is a local inner wall temperature which can be calculated from steady one dimensional heat conduction equation in cylindrical coordinate [28]

$$\frac{1}{r}\frac{d}{dr}\left(kr\frac{dT}{dr}\right) = 0. \tag{5}$$

The solution of this equation with constant heat flux boundary condition at the wall becomes

$$T_{si}(x) = T_{so}(x) - \frac{Q_{\text{conv}} \ln\left(D_o/D_i\right)}{2\pi kL}, \tag{6}$$

where $T_{so}(x)$ represent the local outer wall temperatures, measured by RTD PT 100 type temperature sensors, D_o, D_i are the outer and inner tube diameters, k is the thermal conductivity of the test section wall, and L is the length of the test section.

The average Nusselt number (Nu) can be estimated from the following equation:

$$\text{Nu} = \frac{h_{\text{avg}} D_i}{k_f}. \tag{7}$$

The average heat transfer coefficient can be determined from (7):

$$h_{\text{avg}} = \frac{q_s''}{\left(\widetilde{T}_s - T_b\right)}. \tag{8}$$

The pressure drop (Δp) measured across the test section was used to calculate friction factor (f) using the following equation:

$$f_D = \frac{2\Delta p D_i}{L\rho u^2}. \tag{9}$$

The performance evaluation analysis for laminar flow at the same pumping power is given by the following correlation proposed by Usui et al. [29]:

$$\eta = \frac{\left(\text{Nu}/\text{Nu}_o\right)}{\left(f/f_o\right)^{0.1666}}, \tag{10}$$

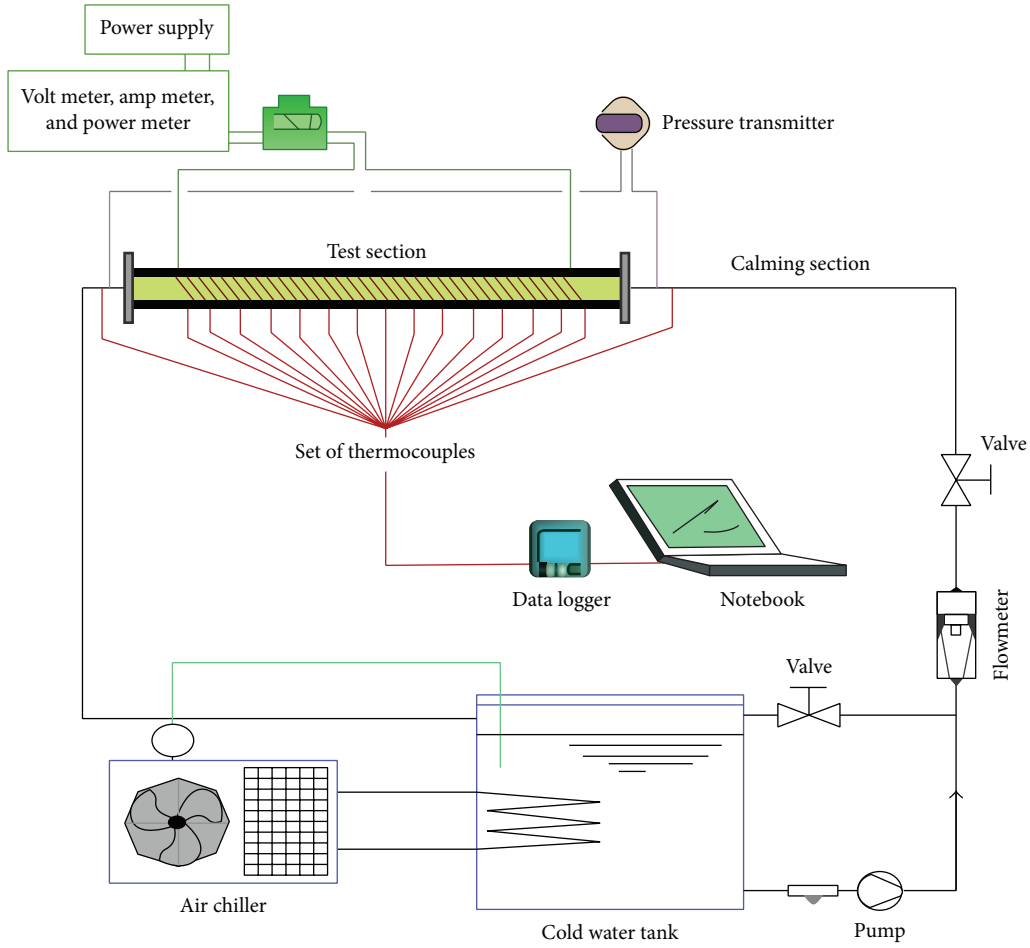

Figure 7: Schematic diagram of the experimental setup.

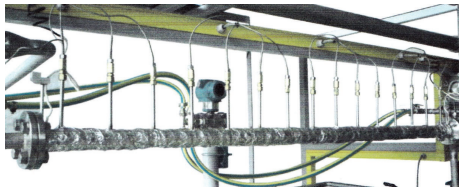

Figure 8: Test section with thermocouple locations.

where Nu and f are, respectively, the Nusselt number and friction factor of the tube with enhancing factor (nanofluid and/or twisted tape) while Nu_o and f_o are, respectively, the Nusselt number and friction factor of the plain tube.

A standard uncertainty analysis was conducted for each measurement using Kline-McClintock method [30]. The maximum uncertainties for Reynolds number, Nusselt number, and friction factor were calculated to be 6.1%, 8.48%, and 2.4%, respectively.

6. Results and Discussions

6.1. Experimental Setup Validation. To evaluate the reliability of the present experimental setup, the experimental results of pure water in plain tube without twisted tape under laminar flow conditions were validated with shah equation [31] and Hagen-Poiseuille equation [28]. The results showed reasonable agreement with the local Nusselt number (Nu_x) and friction factor (f) as shown in Figures 9 and 10:

$$\mathrm{Nu}_x = 1.953 x_*^{-1/3} \quad \text{for } x_* \le 0.03,$$
$$\mathrm{Nu}_x = 4.364 + \frac{0.0722}{x_*} \quad \text{for } x_* > 0.03, \tag{11}$$

$$f = \frac{64}{\mathrm{Re}}. \tag{12}$$

The results of Nusselt number for plain tube with typical twisted tape ($y = 2.93$) were also validated with Manglik and Bergle equation [3]. As shown in Figure 11, the data obtained were found to be in good agreement with the available correlation. For the proof of the present typical twisted tape, Nusselt number of a tube fitted with the present typical twisted tapes was compared with experimental data of right-left helical twist tape [32] as shown in Figures 12 and 13. Apparently, the typical twist tape offered an additional heat transfer enhancement with less skin friction factor.

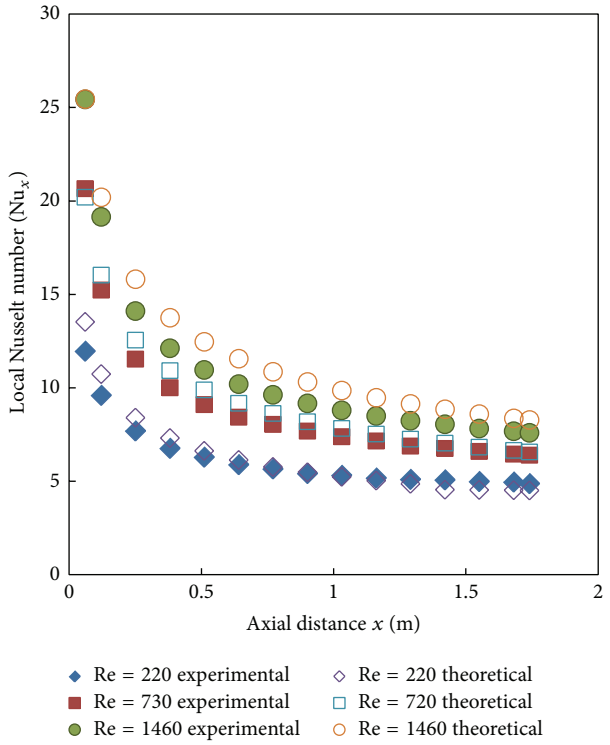

Figure 9: Comparison between measured and calculated local Nusselt number (Nu_x) using DI-Water.

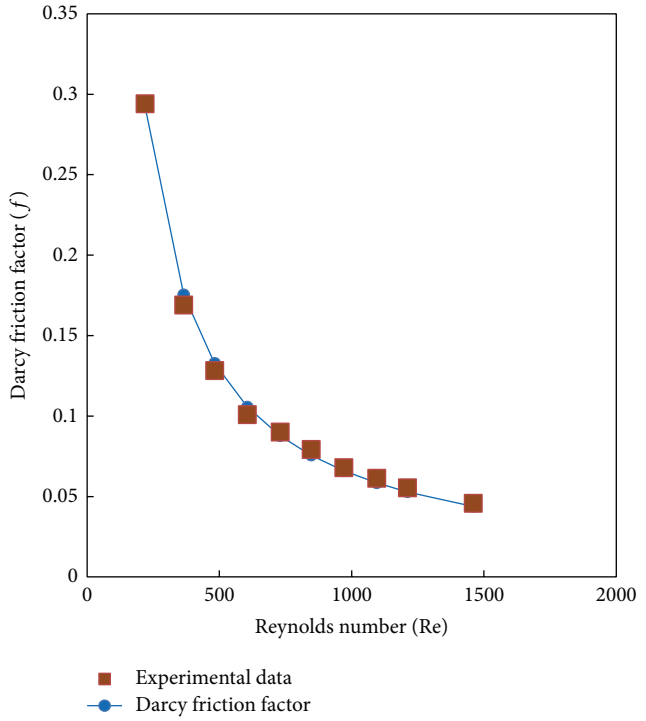

Figure 10: Friction factor across the test section using DI-water as the working fluid.

6.2. Effect of Nanoparticle Volume Concentration in Plain Tube. Experiments were performed to study heat transfer enhancements in plain tube with laminar flow of deionized water and SiO_2 and TiO_2 nanofluids of 1% and 2% volume concentration. The obtained results of Nusselt number and friction factor are elaborated in Figures 14 and 15. From Figure 14, it can be seen that the Nusselt number increased with the increase of nanoparticle concentration and Reynolds number. This means that the presence of nanoparticles increases the energy exchange rates in the fluid with penalty on the wall shear stress due to Brownian motion [33]; the increases of Reynolds number increase random movements of the fluid and consequently enhance the thermal dispersion of the flow. Evidently, SiO_2 nanofluid with 2% volume concentration offered highest Nusselt number, followed by TiO_2 and water, respectively. On other hand, Figure 15 shows slightly augmentation in friction factor value with increases of nanoparticles concentration. This means that the presence of nanoparticles volume fraction increases nanofluid viscosity with wall shear stress. The experimental results were used to derive the following correlations of Nusselt number and friction for water ($\phi = 0$), SiO_2 and TiO_2 nanofluids ($\phi \leq 2\%$). The predicted values of these correlations show reasonable agreement with the experimental results as shown in Figures 16 and 17.

For SiO_2 nanofluid,

$$\mathrm{Nu} = 0.6116\mathrm{Pr}^{0.4}\mathrm{Re}^{0.2795}\left(1+\phi\right)^{3.47}, \quad (13)$$

$$f = 63.236\mathrm{Re}^{-0.994}\left(1+\phi\right). \quad (14)$$

For TiO_2 nanofluid,

$$\mathrm{Nu} = 0.6116\mathrm{Pr}^{0.4}\mathrm{Re}^{0.2795}\left(1+\phi\right)^{1.47}, \quad (15)$$

$$f = 63.236\mathrm{Re}^{-0.994}\left(1+\phi\right). \quad (16)$$

6.3. Effect of Nanoparticle Volume Concentration with Twist Tape. Variations of Nusselt number and friction factor versus Reynolds number for laminar flow of deionized water, SiO_2 and TiO_2 nanofluids of 1% and 2% volume concentration in tube fitted with typical twist tape ($y = 2.93$) are shown in Figures 18 and 19. Evidently, Figure 18 shows that the combined use of nanofluid with twist tape produces further augment in heat transfer coefficient than either nanofluid or twist tape individually. The simultaneous use of nanofluid with twist tape increases the thermal conductivity and viscosity of working fluid as well as increasing swirl flow path. Thus, greater fluid mixing and higher heat transfer coefficient are produced. Eventually, SiO_2 nanofluid with 2% volume concentration with typical twist tape offered a higher Nusselt number compared with the others. As shown in Figure 19, the friction factor decreases with the increase of Reynolds number for water and different volume fractions of nanoparticles. Based on the experimental results, the following correlations of Nusselt number and friction factor were derived. The correlations are valid for laminar flow ($\mathrm{Re} < 1500$), $\phi \leq 2\%$ volume concentration ($\phi = 0$ for water) of SiO_2 and TiO_2 nanofluid, and typical twist tape of twist ratio $y = 2.93$. The predicted data were in good agreement

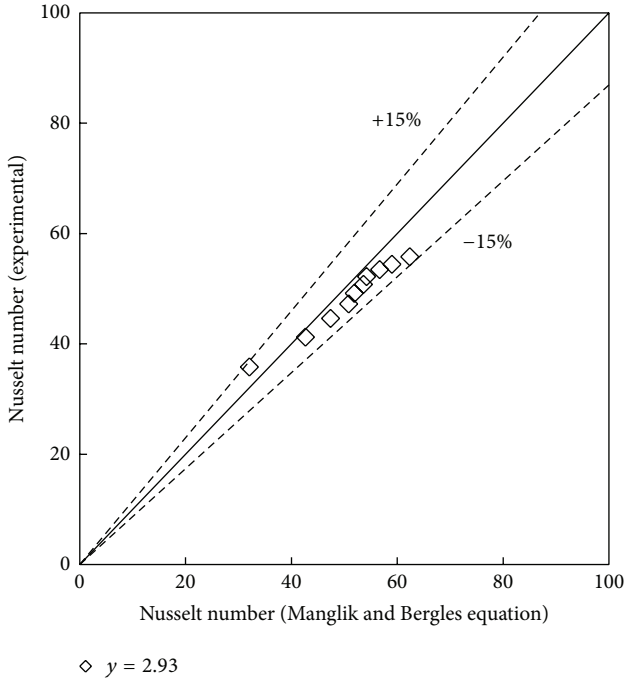

Figure 11: Comparison of experimental and predicted Nusselt number of the plain tube fitted with typical twisted tape.

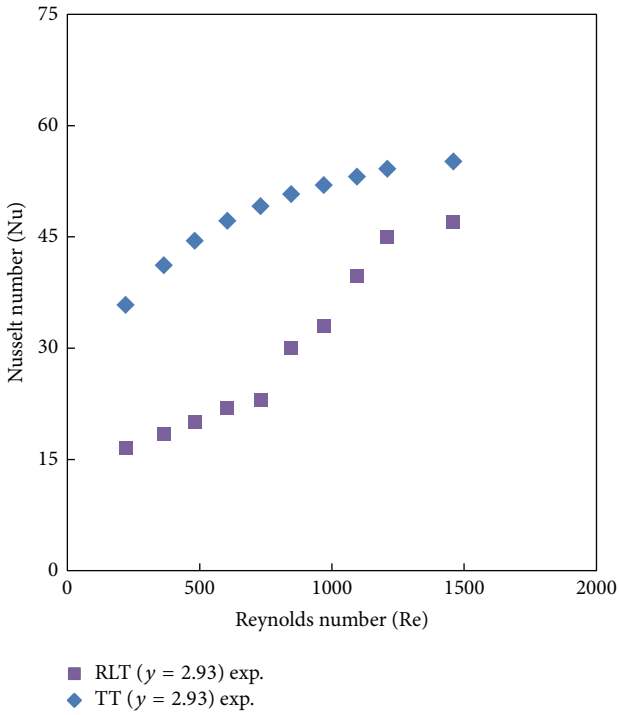

Figure 12: Experimental Nusselt number of typical twist tape with RLT inserts.

with the experimental data within ±6% for Nusselt number and ±8% friction factor as shown in Figures 20 and 21:

$$\mathrm{Nu} = 5.236\mathrm{Pr}^{0.4}\mathrm{Re}^{0.2357}y^{-0.0881}(1+\phi)^{0.124} \quad (17)$$

$$f = 76.789\mathrm{Re}^{-0.686}y^{-0.375}(1+\phi)^{0.198}. \quad (18)$$

6.4. Effect of Twist Tape Configuration. The influence of and conic (quadrant, parabolic half, and triangular) cut twisted tape of twist ratio $y = 2.93$ and cut depth $d_e = 0.5$ cm with 2% volume concentration of SiO_2 nanofluid on Nusselt number and friction factor are shown in Figures 22 and 23. Apparently from Figure 22, conic cut twist exhibits higher Nusselt number than the typical twisted tape. This can be explained by the fact that conic cut twist tape generates swirl flow with efficient fluid mixing nearby their alternative cuts while the typical twist tape causes swirl flow only. The results also reveal that the triangular cut twisted tape provides a higher Nusselt number compared with the others. This means that the vortices behind the alternative cut edges of triangular cut twist tape give superior efficient fluid mixing resulting in further heat transfer enhancement. From Figure 23, it can be seen that friction factor decreases with the increase of Reynolds number and triangular cut twisted tape (VCT) gives higher friction factor compared with all the other Reynolds numbers. This implies that the influence of alternative cuts along the edge of the triangular cut twisted tape promotes additional wall shear stress due to flow mixing between the fluids at the twist tape and tube wall. In addition, the experimental data of conic cut twisted tapes with water ($\phi = 0$) and nanofluids ($\phi = 2\%$) were used to develop the following correlations for Nusselt number and friction factor with reasonable agreement as shown in Figures 24 and 25.

For triangular cut twisted tape,

$$\mathrm{Nu} = 5.387\mathrm{Pr}^{0.4}\mathrm{Re}^{0.229}\left(1+\frac{w}{W}\right)^{0.0383}\left(1+\frac{d_e}{W}\right)^{-0.185} \cdot (1+\phi)^{0.025}, \quad (19)$$

$$f = 61.84\mathrm{Re}^{-0.67}\left(1+\frac{w}{W}\right)^{0.127}\left(1+\frac{d_e}{W}\right)^{-0.468} \cdot (1+\phi)^{0.137}. \quad (20)$$

For parabolic half cut twisted tape,

$$\mathrm{Nu} = 5.388\mathrm{Pr}^{0.4}\mathrm{Re}^{0.229}\left(1+\frac{w}{W}\right)^{0.0384}\left(1+\frac{d_e}{W}\right)^{-0.184} \cdot (1+\phi)^{0.025}, \quad (21)$$

$$f = 68.76\mathrm{Re}^{-0.67}71\left(1+\frac{w}{W}\right)^{0.137}\left(1+\frac{d_e}{W}\right)^{-0.197} \cdot (1+\phi)^{0.0134}. \quad (22)$$

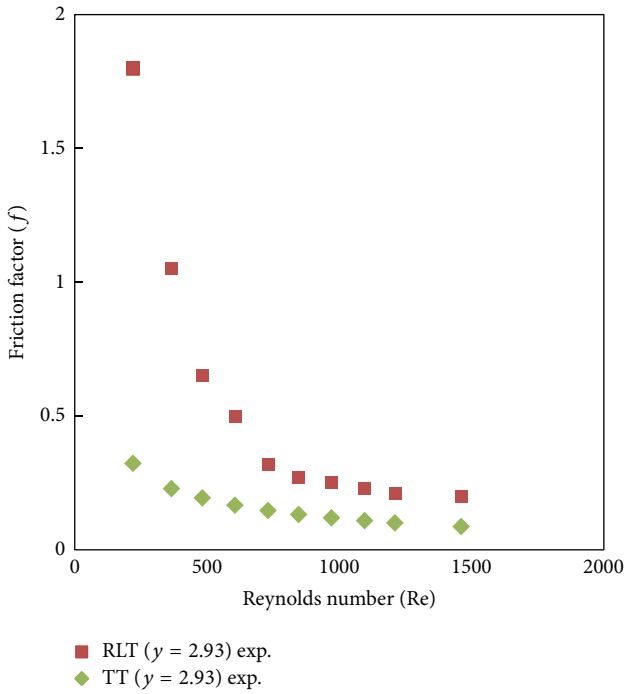

Figure 13: Experimental friction factor of typical twist tape with RLT inserts.

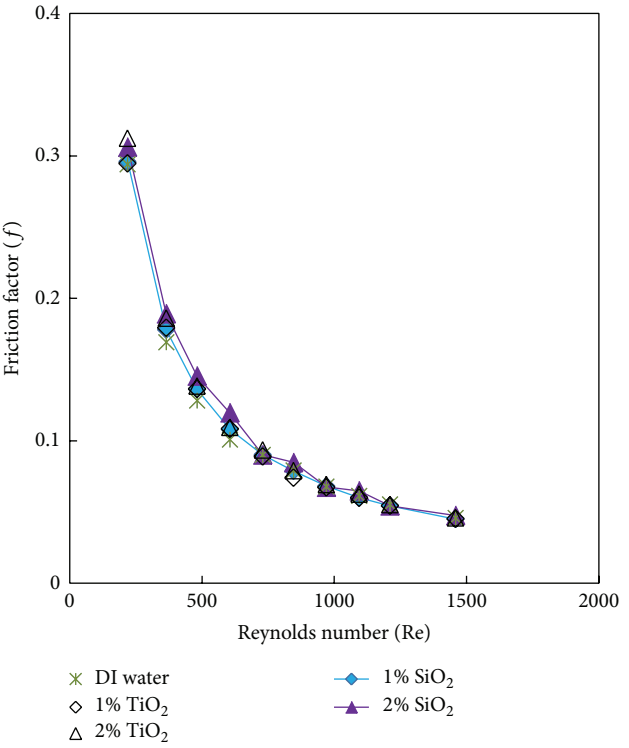

Figure 15: Friction factor versus Reynolds number for plain tube with nanofluids.

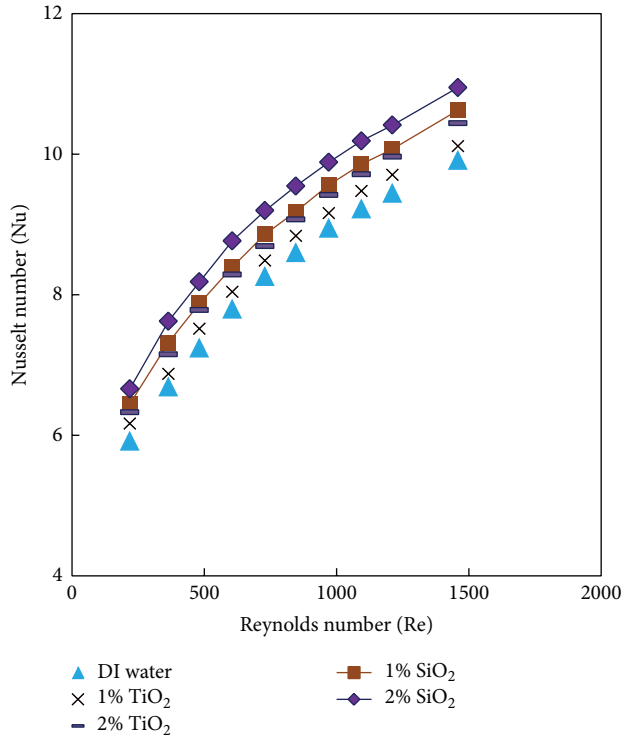

Figure 14: Nusselt number versus Reynolds number for plain tube with nanofluids.

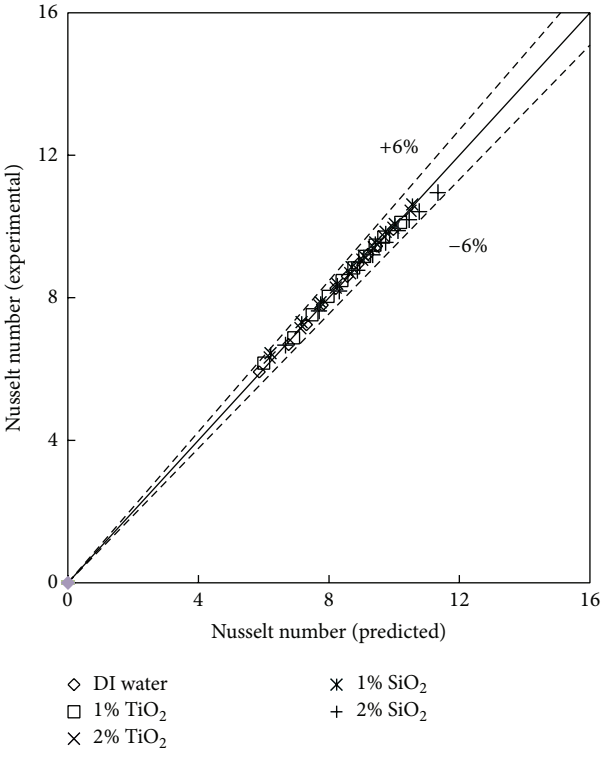

Figure 16: Comparison of experimental and predicted Nusselt number for plain tube.

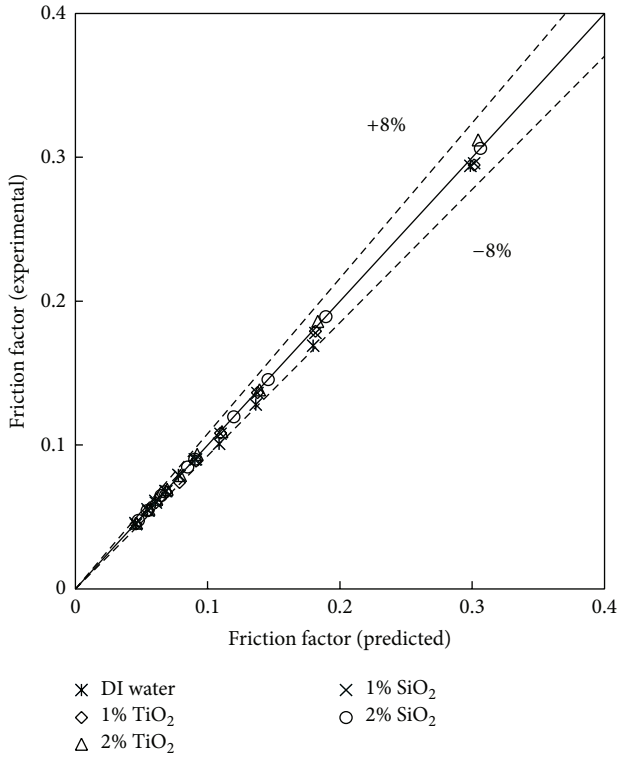

Figure 17: Comparison of experimental and predicted friction factor for plain tube.

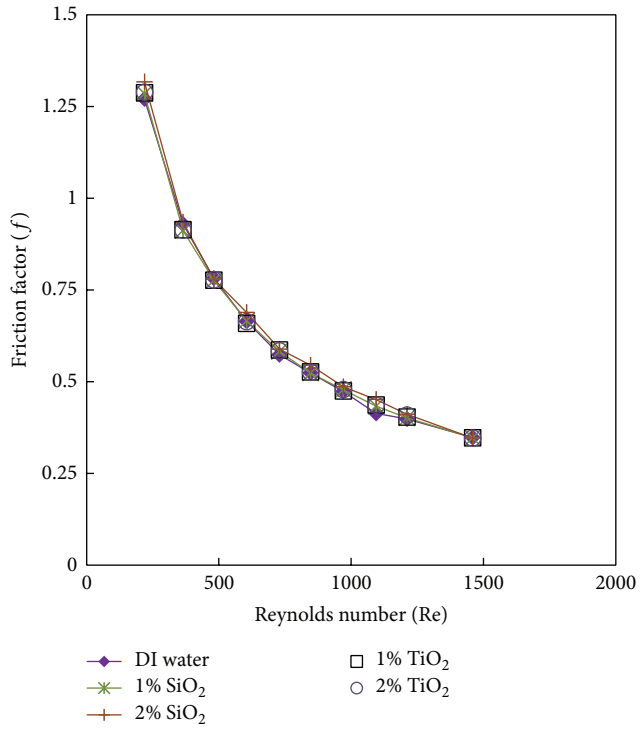

Figure 19: Nusselt number versus Reynolds number for nanofluids with typical twist tape ($y = 2.93$).

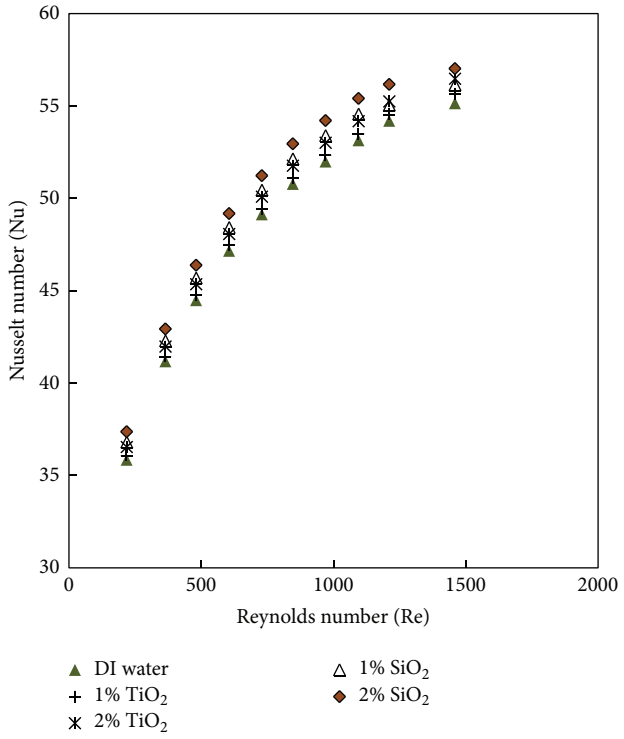

Figure 18: Nusselt number versus Reynolds number for nanofluids with typical twist tape ($y = 2.93$).

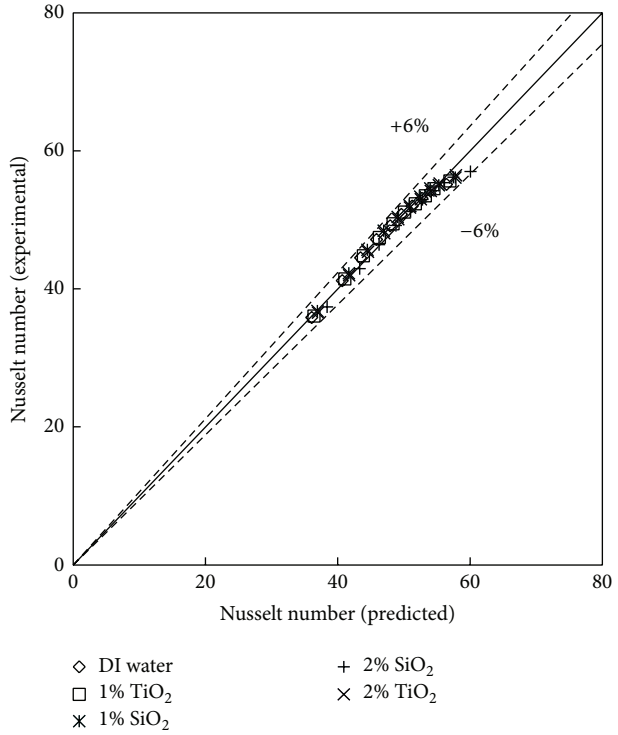

Figure 20: Comparison of experimental and predicted Nusselt number with typical twist tape.

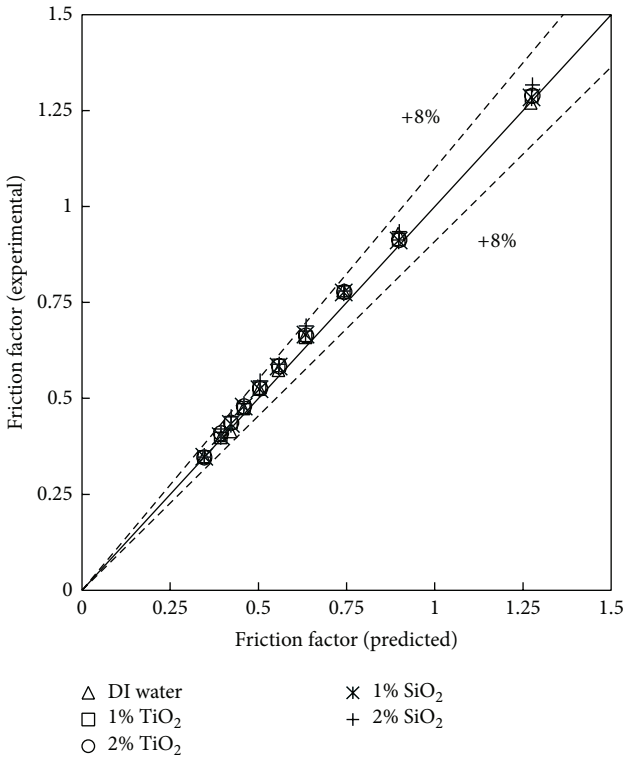

Figure 21: Comparison of experimental and predicted friction factor with typical twist tape.

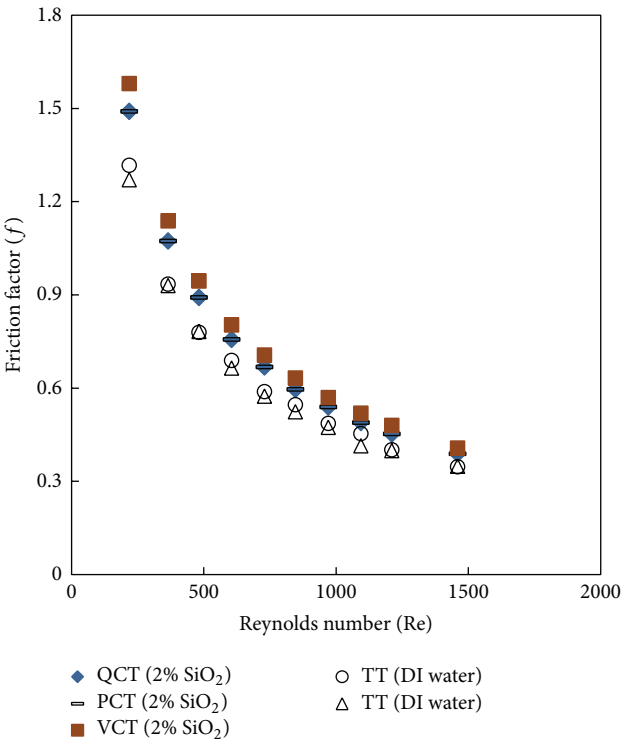

Figure 23: Friction factor versus Reynolds number for typical and conic cut twist tapes.

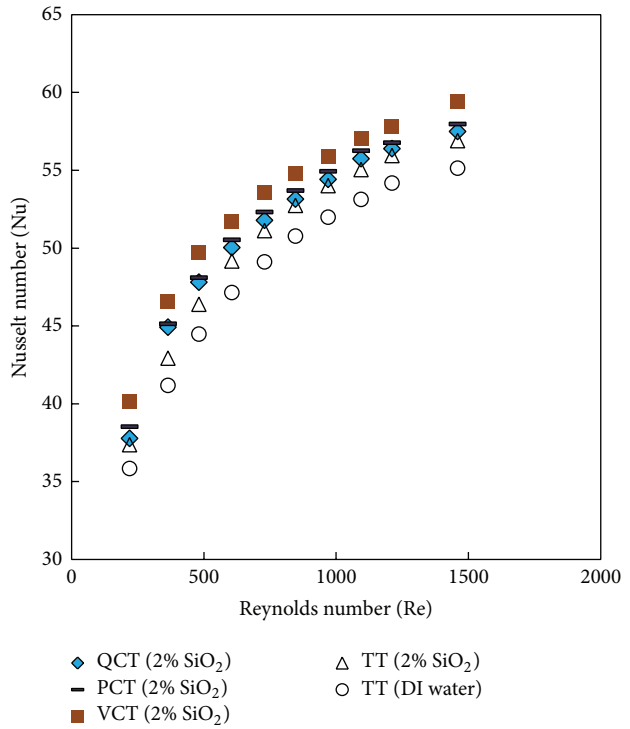

Figure 22: Nusselt number versus Reynolds number for typical and conic cut twist tapes.

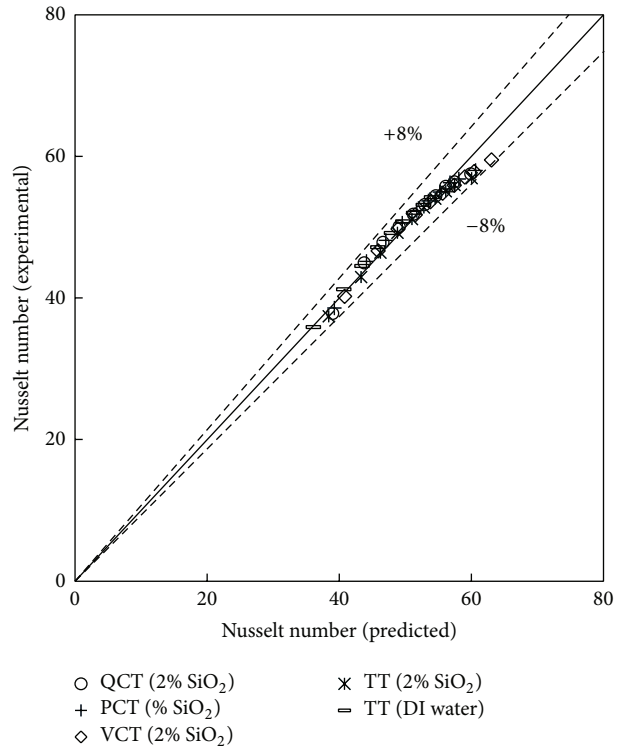

Figure 24: Comparison of experimental and predicted Nusselt number for typical and conic cut twist tapes.

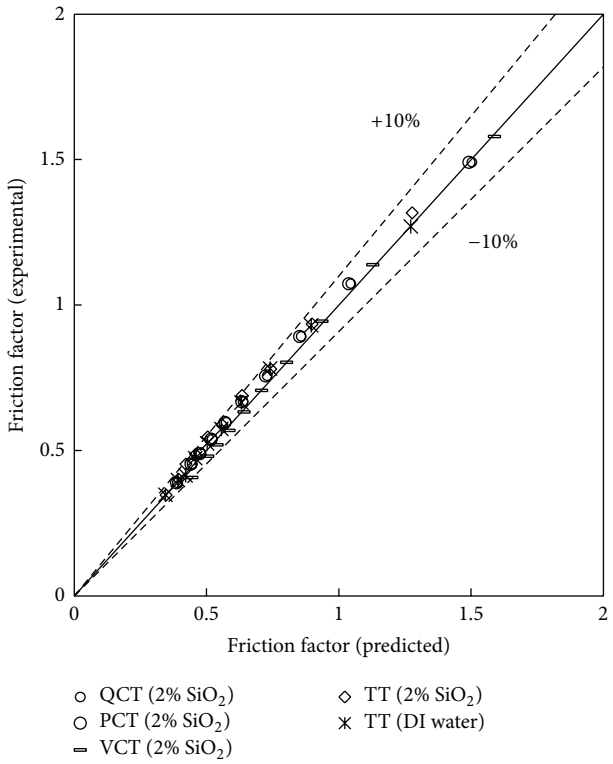

Figure 25: Comparison of experimental and predicted friction factor for typical and conic cut twist tapes.

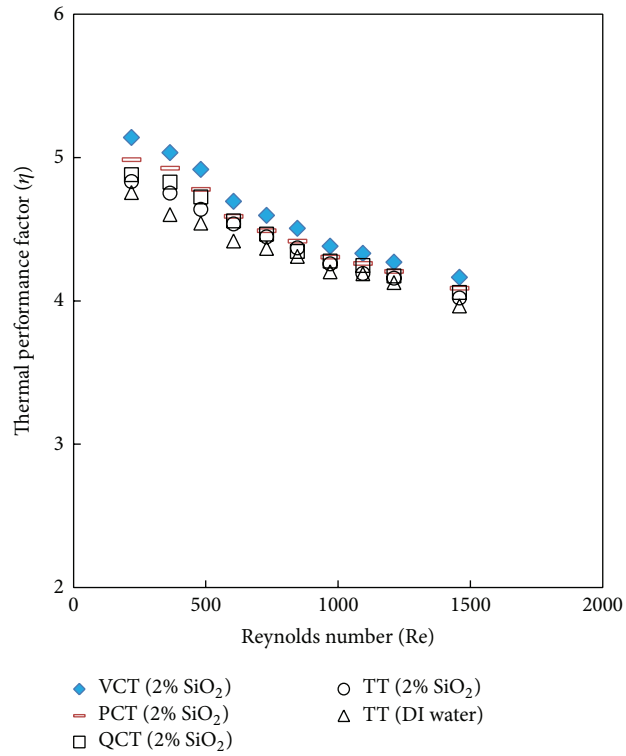

Figure 26: Variation of the thermal performance factor of typical and conic cut twist tape.

For quadrant cut twisted tape,

$$\mathrm{Nu} = 5.38\mathrm{Pr}^{0.4}\mathrm{Re}^{0.226}\left(1+\frac{w}{W}\right)^{0.0387}\left(1+\frac{d_e}{W}\right)^{-0.187} \cdot (1+\phi)^{0.027}, \quad (23)$$

$$f = 69.13\mathrm{Re}^{-0.71}\left(1+\frac{w}{W}\right)^{0.127}\left(1+\frac{d_e}{W}\right)^{-0.16} \cdot (1+\phi)^{0.31}. \quad (24)$$

6.5. Thermal Performance of Twist Tapes. The performance analysis of typical and conic cut twisted tape inserts in laminar flow of SiO_2 nanofluid was accomplished by evaluating thermal performance factor for constant pumping power condition. Thermal performance factor (η) at constants pumping power is defined as ratio of the convective heat transfer coefficient of the tube with turbulator or enhancing method to that of the plain tube. The following thermal performance factor for laminar proposed by [29] is used for performance analysis:

$$\eta = \frac{(\mathrm{Nu}/\mathrm{Nu}_o)}{(f/f_o)^{0.1666}}, \quad (25)$$

where Nu, f, Nu_o, and f_o are the Nusselt numbers and friction factors for a duct configuration with and without inserts, respectively.

Figure 26 shows the variation of thermal performance factor with Reynolds number for 2% volume concentration of SiO_2 nanofluid. The values of thermal performance factor at all Reynolds were found to be greater than unity for both typical and conic cut twisted tape inserts. This indicates that twist tape inserts are feasible in terms of energy saving in laminar flow regime. It is evident that the thermal performance factor triangular cut twist tape at constant Reynolds number is higher than other twist tapes. This is due to the stronger turbulence/swirl flow generated by alternative cuts along the edge twist tape. The thermal performance factor was found to be decreasing with increases in Reynolds number. This is because of the increase in pressure loss as the Reynolds number increases.

The experimental results showed that the thermal performance factor is around 5.13–4.16 for VCT, 4.98–4.08 for PCT, 4.88–4.05 for QCT, and 4.83–4.01 for TT when used with 2% SiO_2 nanofluid. While the thermal performance factor to be around 4.75–3.96 for TT with water. Therefore, the VCT insert shows better thermal performance when used with SiO_2 nanofluid than other twist tapes. The experimental results are used to derive the following correlations of thermal performance factor using least square method of regression analysis. These correlations are valid for laminar flow ($\mathrm{Re} < 1500$) of water and 2% volume concentration SiO_2 for typical and conic cut twist tapes. The comparisons between the thermal performance factor values obtained from experimental data and those predicted from the above correlations are

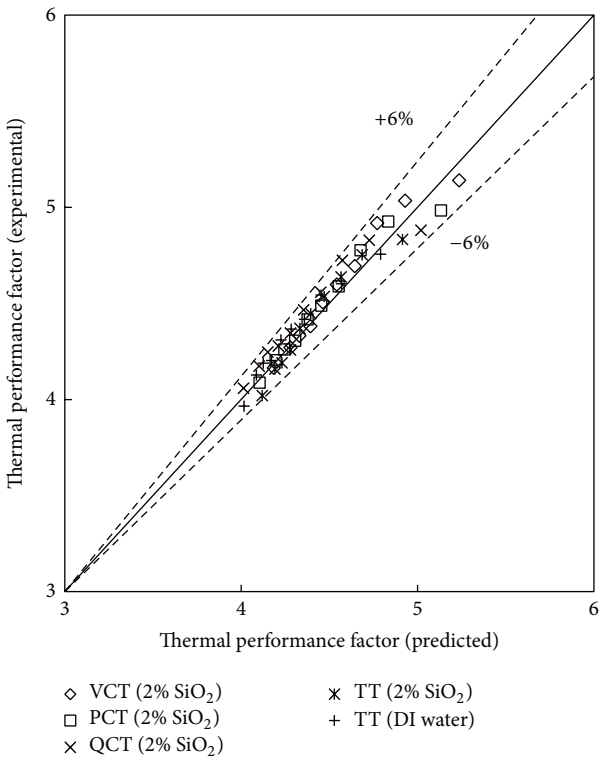

Figure 27: Comparison of experimental and predicted thermal performance for typical and conic cut twist tapes.

shown in Figure 27. As shown, the predicted data are in good agreement with the experimental data.

For VCT twisted tape,

$$\eta = 5.173\mathrm{Re}^{-0.118}\left(1+\frac{w}{W}\right)^{2.483}\left(1+\frac{d_e}{W}\right)^{-0.247} \cdot \left(1+\phi_{\mathrm{SiO}_2}\right)^{0.0183}. \quad (26)$$

For PCT twisted tape,

$$\eta = 5.173\mathrm{Re}^{0.0945}\left(1+\frac{w}{W}\right)^{3.113}\left(1+\frac{d_e}{W}\right)^{-0.247} \cdot \left(1+\phi_{\mathrm{SiO}_2}\right)^{0.0183}. \quad (27)$$

For QCT twisted tape,

$$\eta = 5.173\mathrm{Re}^{0.118}\left(1+\frac{w}{W}\right)^{3.49}\left(1+\frac{d_e}{W}\right)^{-0.247} \cdot \left(1+\phi_{\mathrm{SiO}_2}\right)^{0.0183}. \quad (28)$$

For TT twisted tape with SiO nanofluid,

$$\eta = 7.91\mathrm{Re}^{0.0.93}\left(1+\phi_{\mathrm{SiO}_2}\right)^{1.283}. \quad (29)$$

For TT twisted tape with deionized water,

$$\eta = 7.91\mathrm{Re}^{0.0.93}. \quad (30)$$

7. Conclusions

Heat transfer, friction, and thermal performance characteristics of SiO_2 and TiO_2 nanofluids with two concentrations of 1% and 2% by volume in a circular tube fitted with a typical and conic cut twist tape in the laminar regime have been experimentally investigated. The main conclusions from this experimental study are as follows.

(7.1) SiO_2 and TiO_2 nanofluids of different volume concentration in plain tube give good enhancement in Nusselt number compared to deionized water. The higher enhancement in Nusselt number is obtained by SiO_2 nanofluids with volume concentrations of 2%.

(7.2) At similar conditions, the insertion of typical twist tape causes very significant convective heat transfer enhancement in the laminar flow; however, further enhancement is observed by the simultaneous use of nanofluid with twisted tape compared to the use of twisted tape or nanofluid alone.

(7.3) The use of nanofluid with the conic cut twist tape provides a considerably higher Nusselt number than that of nanofluid with the typical twist tape for all Reynolds numbers examined. The triangular cut twist tape offers higher heat transfer rate than the typical twist tape and other conic cut configurations.

(7.4) Over the range investigated (Re = 220–1500), the maximum thermal performance factor of 5.13 is found with the simultaneous use of the triangular twist tape with SiO_2 nanofluid with 2% volume concentration at Reynolds number of 220.

(7.5) The empirical correlations for the Nusselt number, friction factor, and the thermal performance factor for typical and conic cut twist tapes are developed and fitted with the experimental data of water and nanofluids.

Conflict of Interests

The authors declare that there is no conflict of interests regarding the publication of this paper.

Acknowledgments

The authors would like to thank the National University of Malaysia and the Ministry of Higher Education for the financial support (FRGS/1/2013/TK07/UKM/01/1 and DPP-2013-114) to perform this investigation.

References

[1] A. Bejan and A. D. Kraus, *Heat Transfer Handbook*, John Wiley & Sons, 2003.

[2] I. Singh and N. Diwakar, *International Journal of Applied Research in Mechanical Engineering*, vol. 3, pp. 16–29, 2013.

[3] R. M. Manglik and A. E. Bergles, "Heat transfer and pressure drop correlations for twisted-tape inserts in isothermal tubes:

part I—laminar flows," *Journal of Heat Transfer*, vol. 115, no. 4, pp. 881–889, 1993.

[4] S. K. Saha and D. Chakraborty, "Heat transfer and pressure drop characteristics of laminar flow through a circular tube fitted with regularly spaced twisted tape elements with multiple twists," in *Proceedings of the Heat and Mass Transfer Conference*, pp. 313–318, Kanpur, India, 1997.

[5] S. Al-Fahed, L. M. Chamra, and W. Chakroun, "Pressure drop and heat transfer comparison for both microfin tube and twisted-tape inserts in laminar flow," *Experimental Thermal and Fluid Science*, vol. 18, no. 4, pp. 323–333, 1998.

[6] M. S. Lokanath and R. D. Misal, "An experimental study on the performance of plate heat exchanger and an augmented shell and tube heat exchanger for different types of fluids for marine applications," in *Proceedings of the 5th ISHMT-ASME Heat and Mass Transfer Conference*, pp. 863–868, Tata McGraw-Hill, New Delhi, India, 2002.

[7] P. Sivashanmugam and S. Suresh, "Experimental studies on heat transfer and friction factor characteristics of laminar flow through a circular tube fitted with helical screw-tape inserts," *Applied Thermal Engineering*, vol. 26, no. 16, pp. 1990–1997, 2006.

[8] P. Sivashanmugam and S. Suresh, "Experimental studies on heat transfer and friction factor characteristics of laminar flow through a circular tube fitted with regularly spaced helical screw-tape inserts," *Experimental Thermal and Fluid Science*, vol. 31, no. 4, pp. 301–308, 2007.

[9] S. Jaisankar, T. K. Radhakrishnan, and K. N. Sheeba, "Studies on heat transfer and friction factor characteristics of thermosyphon solar water heating system with helical twisted tapes," *Energy*, vol. 34, no. 9, pp. 1054–1064, 2009.

[10] A. V. N. Kapatkar, B. D. A. S. Padalkar, and C. S. Kasbe, "Experimental investigation on heat transfer enhancement in laminar flow in circular tube equipped with different inserts," *AMAE International Journal on Manufacturing and Material Science*, vol. 1, pp. 1–6, 2011.

[11] J. Guo, A. Fan, X. Zhang, and W. Liu, "A numerical study on heat transfer and friction factor characteristics of laminar flow in a circular tube fitted with center-cleared twisted tape," *International Journal of Thermal Sciences*, vol. 50, no. 7, pp. 1263–1270, 2011.

[12] K. Wongcharee and S. Eiamsa-ard, "Friction and heat transfer characteristics of laminar swirl flow through the round tubes inserted with alternate clockwise and counter-clockwise twisted-tapes," *International Communications in Heat and Mass Transfer*, vol. 38, no. 3, pp. 348–352, 2011.

[13] E. Z. Ibrahim, "Augmentation of laminar flow and heat transfer in flat tubes by means of helical screw-tape inserts," *Energy Conversion and Management*, vol. 52, no. 1, pp. 250–257, 2011.

[14] S. U. S. Choi and J. A. Eastman, "Enhancing thermal conductivity of fluids with nanoparticles," in *Developments and Applications of Non-Newtonian Flows*, D. A. Siguier and H. P. Wang, Eds., pp. 99–105, American Society of Mechanical Engineers, New York, NY, USA, 1995.

[15] C. Y. Tsai, H. T. Chien, P. P. Ding, B. Chan, T. Y. Luh, and P. H. Chen, "Effect of structural character of gold nanoparticles in nanofluid on heat pipe thermal performance," *Materials Letters*, vol. 58, no. 9, pp. 1461–1465, 2004.

[16] M.-S. Liu, M. C.-C. Lin, C. Y. Tsai, and C.-C. Wang, "Enhancement of thermal conductivity with Cu for nanofluids using chemical reduction method," *International Journal of Heat and Mass Transfer*, vol. 49, no. 17-18, pp. 3028–3033, 2006.

[17] E. Tamjid and B. H. Guenther, "Rheology and colloidal structure of silver nanoparticles dispersed in diethylene glycol," *Powder Technology*, vol. 197, no. 1-2, pp. 49–53, 2010.

[18] S. M. S. Murshed, K. C. Leong, and C. Yang, "Enhanced thermal conductivity of TiO_2 water based nanofluids," *International Journal of Thermal Sciences*, vol. 44, no. 4, pp. 367–373, 2005.

[19] H. Zhu, C. Zhang, S. Liu, Y. Tang, and Y. Yin, "Effects of nanoparticle clustering and alignment on thermal conductivities of Fe_3O_4 aqueous nanofluids," *Applied Physics Letters*, vol. 89, Article ID 023123, 2006.

[20] J. A. Eastman, U. S. Choi, S. Li, L. J. Thompson, and S. Lee, "Enhanced thermal conductivity through the development of nanofluids," *MRS Proceedings*, vol. 457, 1996.

[21] M. E. Meibodi, M. Vafaie-Sefti, A. M. Rashidi, A. Amrollahi, M. Tabasi, and H. S. Kalal, "Simple model for thermal conductivity of nanofluids using resistance model approach," *International Communications in Heat and Mass Transfer*, vol. 37, no. 5, pp. 555–559, 2010.

[22] G. Pathipakka and P. Sivashanmugam, "Heat transfer behaviour of nanofluids in a uniformly heated circular tube fitted with helical inserts in laminar flow," *Superlattices and Microstructures*, vol. 47, no. 2, pp. 349–360, 2010.

[23] K. Wongcharee and S. Eiamsa-ard, "Enhancement of heat transfer using CuO/water nanofluid and twisted tape with alternate axis," *International Communications in Heat and Mass Transfer*, vol. 38, no. 6, pp. 742–748, 2011.

[24] S. Suresh, K. P. Venkitaraj, and P. Selvakumar, "Comparative study on thermal performance of helical screw tape inserts in laminar flow using Al_2O_3/water and CuO/water nanofluids," *Superlattices and Microstructures*, vol. 49, no. 6, pp. 608–622, 2011.

[25] S. D. Salman, A. A. H. Kadhum, M. S. Takriff, and A. B. Mohamad, "Heat transfer enhancement of laminar nanofluids flow in a circular tube fitted with parabolic-cut twisted tape inserts," *The Scientific World Journal*, vol. 2014, Article ID 543231, 7 pages, 2014.

[26] S. D. Salman, A. A. H. Kadhum, M. S. Takriff, and A. B. Mohamad, "CFD simulation of heat transfer and friction factor augmentation in a circular tube fitted with elliptic-cut twisted tape inserts," *Mathematical Problems in Engineering*, vol. 2013, Article ID 163839, 7 pages, 2013.

[27] S. D. Salman, A. A. H. Kadhum, M. S. Takriff, and A. B. Mohamad, "CFD analysis of Heat transfer and friction factor characteristics in a circular tube fitted with Quadrant-cut twisted tape inserts," *Mathematical Problems in Engineering*, vol. 2013, Article ID 273764, 8 pages, 2013.

[28] F. P. Incropera, D. P. Dewitt, T. L. Bergman, and A. S. Lavine, *Fundamentals of Heat and Mass Transfer*, John Wiley & Sons, 2007.

[29] H. Usui, Y. Sano, K. Iwashita, and A. Isozaki, "Enhancement of heat transfer by a combination of internally grooved rough tube and twisted tape," *International Chemical Engineering*, vol. 26, no. 1, pp. 97–104, 1986.

[30] J. P. Holman, *Experimental Methods for Engineers*, McGraw-Hill, New York, NY, USA, 2011.

[31] R. K. Shah and A. L. London, *Laminar Flow Forced Convection in Ducts*, Academic Press, New York, NY, USA, 1978.

[32] P. K. Nagarajan and P. Sivashanmugam, "CFD simulation of heat transfer augmentation in a circular tube fitted with right-left helical inserts with spacer," *International Journal of Chemical Engineering Research*, vol. 1, pp. 1–11, 2009.

[33] P. Keblinski, S. R. Phillpot, S. U. S. Choi, and J. A. Eastman, "Mechanisms of heat flow in suspensions of nano-sized particles (nanofluids)," *International Journal of Heat and Mass Transfer*, vol. 45, no. 4, pp. 855–863, 2002.